NANO LETTERS

2003
Vol. 3, No. 5
577−580

Synthesis, Characterization, and Manipulation of Helical SiO_2 Nanosprings

Hai-Feng Zhang,[†,‡] Chong-Min Wang,[‡] Edgar C. Buck,[‡] and Lai-Sheng Wang*[,†,‡]

Department of Physics, Washington State University, 2710 University Drive, Richland, Washington 99352, and W. R. Wiley Environmental Molecular Sciences Laboratory, Pacific Northwest National Laboratory, P.O. Box 999, Richland, Washington 99352

Received February 28, 2003; Revised Manuscript Received March 13, 2003

ABSTRACT

Amorphous helical SiO_2 nanosprings (80 to 140 nm in diameter and up to 8 microns long) were synthesized with a chemical vapor deposition technique, characterized and manipulated by scanning (SEM) and transmission (TEM) electron microscopy and atomic force microscopy (AFM). The helical nanosprings were observed in the middle of a straight nanowire and were formed by a perturbation during the growth of the straight nanowire. Contraction and expansion of the helical nanosprings were observed under in situ electron beam heating during TEM, as well as bending induced by an AFM tip, suggesting that the helical nanosprings are highly flexible and may have potential applications in nanomechanical, nanoelectronmagnetic devices, and composite materials.

Helical nanosprings represent a new variety among the family of one-dimensional nanostructures, which have attracted great attention in nanoscience recently.[1−3] In addition to their anticipated structural flexibility, helical nanosprings present additional opportunities for nano-engineering, such as helicity and periodicity. Heretofore only a few helical nanostructures have been observed,[4−10] and it has been challenging to devise high yield and controlled synthesis of uniform helical nanostructures. There has been no physical characterization of the potentially novel properties of this new nanostructure. Here we report the facile synthesis of helical silica nanosprings using a chemical vapor deposition (CVD) technique and physical characterization and manipulation using scanning (SEM), transmission (TEM) electron microscopy, and atomic force microscopy (AFM). The helical silica nanosprings synthesized range from 80 to 140 nm in diameter and several microns in length with variable periodicity. Stretching and contraction of the helical silica nanosprings were observed under in situ electron beam heating in TEM, as well as bending by an AFM tip. Springs are important mechanical devices found in many applications.[11] Silica glass springs in particular have been used for their low thermal expansion and contraction in comparison with that of metals.[12] Helical silica nanosprings may have potential applications in nanomechanical, -electronic, -electromagnetic systems, and composite materials.

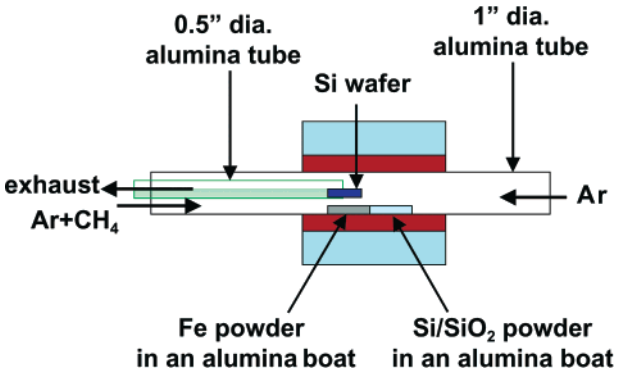

Figure 1. Programmable temperature controlled tube furnace. During reaction, the Ar carrier gas was allowed to flow into the tube from both ends and exhaust out from the inner ceramic tube. Iron powder and SiO_2/Si mixed powder were loaded in two sample boats located near the center of the furnace right below the Si wafer. CH_4 was added into the Ar carrier gas on the left side of the furnace.

The helical SiO_2 nanosprings were synthesized in a dual flow-tube furnace (Figure 1). The inner alumina tube was positioned at the center of the furnace inside the outer tube and held the Si wafer, on which the SiO_2 nanostructures were grown. Iron and Si/SiO_2 (1:1 molar ratio) powders in two separate alumina sample boats were placed right beneath the Si wafer inside the outer flow tube. Carrier gases could flow from both ends of the outer tube and exhaust through the

* Corresponding author. E-mail: ls.wang@pnl.gov
† Washington State University.
‡ Pacific Northwest National Laboratory.

10.1021/nl0341180 CCC: $25.00
Published on Web 04/04/2003

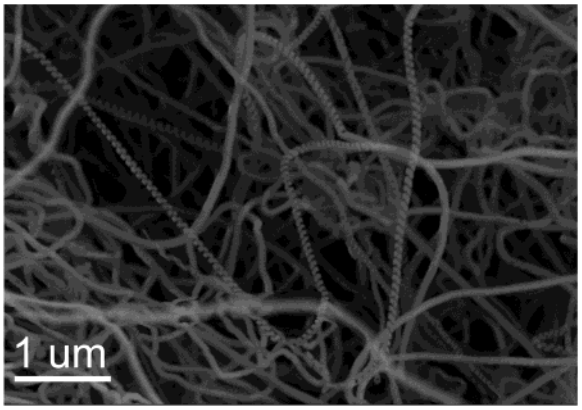

Figure 2. SEM characterization of as-synthesized silicon oxide nanowires. A LEO DSM 982 Gemini digital field emission scanning electron microscope was used. The as-synthesized materials consist mainly of nanowires with uniform diameters and up to tens of micrometers long. Among the nanowires, a substantial fraction was found to be of helical morphology with the appearance of ordinary coiled telephone cords.

inner tube. The synthesis took about 2 h under 1160 °C and with a small flow of CH_4,[13] and a thin layer of white fluffy material was observed on the Si substrate. SEM revealed that most of the materials were wire-like structures with diameters in the nanometer size range and tens of microns long (Figure 2). Most surprisingly, we observed a large quantity of helical nanostructures, much like coiled telephone cords, which always seemed to terminate to straight nanowires at their two ends. The diameters of the helical nanostructures were fairly uniform. The distribution of the helical nanowires on the silicon wafer was not homogeneous. Overall, the ratio between the helical nanostructures and the straight ones was about 10−15%.

TEM revealed four kinds of morphologies among the helical nanostructures (Figure 3a−d). Figure 3a shows one end of the junction between a helical and straight nanowire, where an oval-shaped nanoparticle is always observed (inset of Figure 3a). The size of the nanoparticle is much smaller than the diameters of the straight nanowires. Figure 3b shows the typical middle part of the helical nanowire with uniform diameter and periodicity. Figure 3c shows a part toward the other end of the helical nanowire, which exhibits uniform diameter but variable periodicity. Finally, Figure 3d reveals the other end of the junction between the helical and straight nanowire, which has a hollow tube-like structure terminated to a trapped nanoparticle (inset Figure 3d). Energy-dispersive X-ray elemental analyses revealed that the nanoparticles in Figure 3a and Figure 3d are pure Fe, which was also confirmed by the diffraction pattern shown in the inset of Figure 3c. Using high-resolution TEM (HRTEM) and elemental analyses, we found that all the nanowires, both the straight sections and the helical parts, are pure amorphous SiO_2. Chemical mapping images of oxygen and silicon in one section of a helical nanostructure are shown in Figure 3e and f. We found that all the helical nanostructures exhibit similar morphologies as shown in Figure 3a−d, starting from a straight wire to the uniform part of the helical structure, which constitutes the main body of the helical nanostructure,

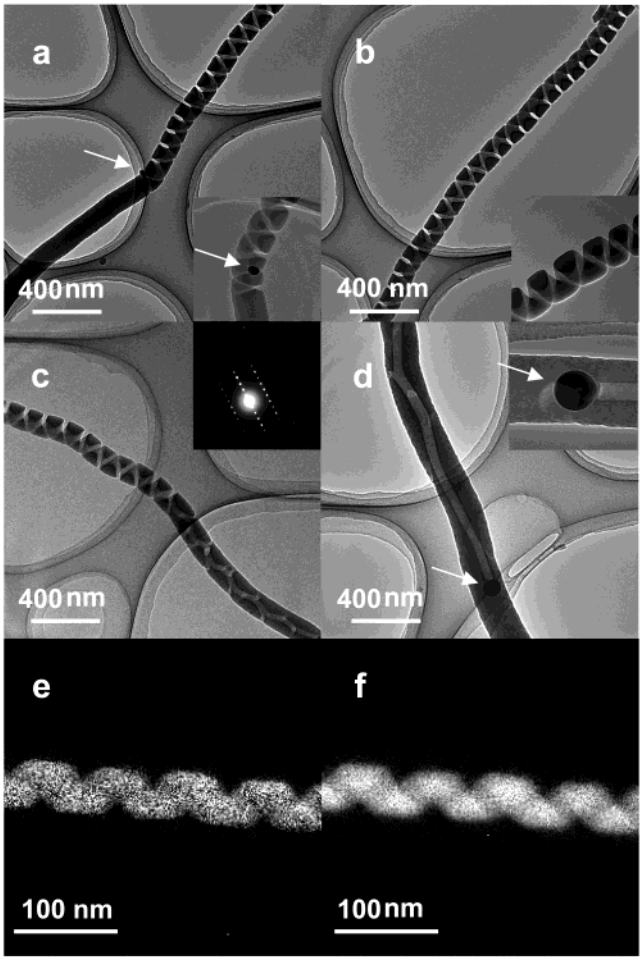

Figure 3. TEM and composition characterization of the helical nanowires. (a) A junction between a straight and helical nanowire. The inset is a high magnification image of the junction part, showing more clearly the oval-shaped nanoparticles (arrows). The diameters of the straight nanowire and the helical structure are the same. (b) The main body of the helical nanostructure. The inset is a high magnification image of the helical structure. (c) The morphology transition from a uniform helical nanostructure to a structure with variable periodicity. The inset is the diffraction pattern of the nanoparticles in (a) and (d), showing that these nanoparticles are crystalline Fe. (d) A junction between a hollow tube and a straight nanowire. A spherical Fe nanoparticle is always found trapped at the end of the hollow tube. The inset shows a higher magnification image of the Fe nanoparticle. (e) and (f) Chemical mappings for oxygen and silicon calculated by the three-window method using pre- and postedge images at the oxygen K-edge and silicon L-edge, respectively. The TEM characterization was performed with a JEOL JEM-2010 instrument operated at 200 keV.

then going through a transition from a uniform period to a variable period (Figure 3c), which eventually turns into a hollow tube terminated to an Fe nanoparticle (Figure 3d).

The cross section of the nanowire forming the helical nanostructure was not cylindrical, but rather rectangular (ribbon-like), as revealed by the triangular shape in the high contrast areas in the HRTEM images (Figure 3a−c). The widths of the ribbon cross sections are similar to the radius of the linear parts, whereas the ribbon thickness appeared to be much smaller. The straight nanowires are quite long, up to tens of micrometers, but the helical parts are shorter − the longest that we observed was up to 8 μm. Most of the

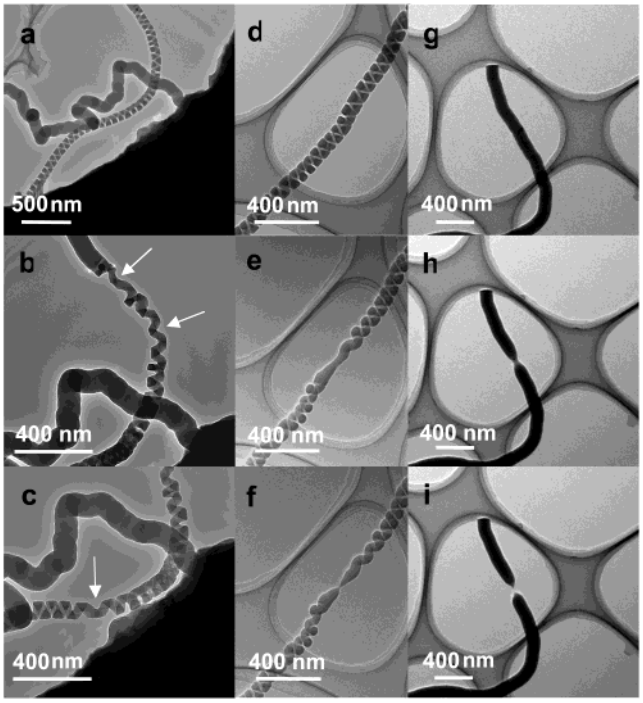

Figure 4. In situ electron beam heating of silica nanostructures. (a) A bent helical nanospring before e-beam heating. (b) The helical nanospring shown in (a) after e-beam heating for about 10 s each at the arrow-pointed spots. Note the stretching of the heated parts and the contraction of the lower part of the nanospring. (c) Electron-beam heating of the lower part of the nanospring. Note the reverse stretching and the bending of the nanospring. (d) A straight helical nanospring prior to e-beam heating. (e) and (f) The helical nanowire shown in (d) after 12 and 27 min e-beam heating. (g) A cylindrical nanowire before e-beam heating. (h) and (i) The nanowire shown in (g) after 15 and 21 min e-beam heating. The beam current used in all the heating experiments was 2 μA.

helical nanowires were tightly wound with only a very small gap (a fraction of the width of the ribbon cross section) between adjacent turns (Figure 3). A small number of the helical nanowires were loose with gaps between adjacent turns larger than the width of the nanowire forming the helical structure. A statistical analysis yielded the mean values for the width of the ribbon cross section, the diameter and pitch of the nanosprings as 67, 102, and 85 nm, respectively (Supporting Information, Figure s1).

One of the unique properties of a spring is its mechanical flexibility and ability to store potential energy when stretched or compressed. Although bulk silica is brittle, the silica nanosprings are expected to be highly flexible nanostructures. To test the flexibility of the silica nanosprings, we performed an in situ heating experiment during TEM imaging by focusing the electron beam on a certain part of the nanosprings. Two different behaviors were observed. Figure 4a shows a bent helical structure near the junction with a straight wire. Figure 4b shows the same nanostructure after the e-beam heating near the junction for about 10 s each at two separate spots, as indicated by the arrows. The helical nanospring clearly expanded at the heated parts, while at the same time the lower part of the nanowires was contracted and further bent. We heated a spot again below the contracted part for about 20 s and observed that it was further expanded and bent (Figure 4c), demonstrating vividly the elasticity of the nanospring.

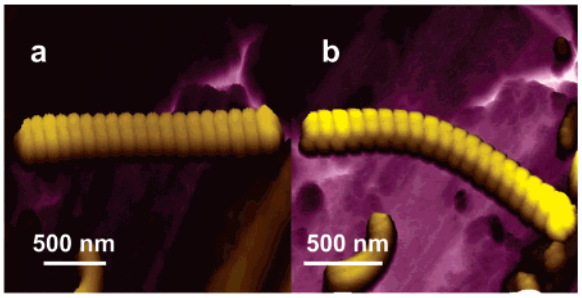

Figure 5. AFM manipulation of a helical silica nanospring. (a) and (b) Before and after AFM manipulation of a section of free-standing helical silica nanospring. The AFM manipulation was performed in air with a Digital Instruments NanoScope III on a sample that had been imaged by TEM. Samples were transferred from the silicon substrate to a carbon-coated Cu grid TEM sample holder simply by scratching the copper grid against the surface of the silicon wafer.

However, when we heated a straight section of a helical nanospring (Figure 4d), no apparent expansion was observed. Instead the shape of the structure was changed (Figure 4e) after a long time exposure to the electron beam ($\sim$12 min) due to melting or evaporation. Continuing heating for about 27 min resulted in rupture of the nanospring (Figure 4f). The different behaviors of the nanosprings in Figure 4a and d under e-beam heating were initially surprising. This observation suggests that the bent nanospring must be under elastic strain, i.e., storing a substantial amount of elastic energy, which helped the stretching of the heated part when it became softer. On the other hand, the straight nanospring should be at its rest state and stored no elastic energy. Upon heating, no stretching would be expected since the thermal expansion was likely to be too small to have any significant influence on the overall length of the nanospring. We further performed a control experiment on a straight cylindrical silica nanowire, which should not contain any elastic energies. We found that the response of the straight nanowire upon e-beam heating (Figure 4g−i) was identical to that of the straight nanospring.

We also examined the flexibility of the helical nanostructures using AFM. Figure 5a displays an AFM image of a section of a free-standing helical silica nanospring on the Cu surface of a TEM grid, revealing the uniform periodicity along its entire length. Figure 5b shows the same nanospring after it was pushed by the AFM tip at one end. The bending and a slight stretching of the helical nanospring observed here indicate again its high flexibility.

Straight and cylindrical SiO_2 nanowires have been fabricated previously using the vapor−liquid−solid (V−L−S) method.[14−18] However, there has been no report of helical SiO_2 nanowires. Several models have been advanced for the formation of helical nanostructures.[5−8] The SiO_2 nanosprings reported here appear to have similar morphology to the amorphous boron carbide nanosprings,[5] for which a growth model involving the contact angle anisotropy between the growing nanowire and the Fe catalytic particle was proposed. A similar V−L−S growth mechanism could be operative for the formation of the amorphous SiO_2 nanosprings, though

the growth conditions are quite different. At 1160 °C, the mixture of Si/SiO_2 reacted to form SiO gaseous molecules [$SiO_2 + Si \rightarrow 2SiO(g)$], which were carried to the Si wafer located at the entrance of the inner tube (Figure 1). There the SiO gas molecules reacted with Si to form the silica nanowires via the V−L−S process with Fe catalytic particles. The role of CH_4 during the growth is not known, but it is important because without the CH_4 flow no helical nanostructures were observed. Elemental mapping of carbon only revealed trace amount of carbon in the SiO_2 nanostructures. We suspect that the CH_4 helps moderate the highly oxidizing environment and maintain the catalytic effects of the Fe particles.

Chemical vapor deposition is the most plausible technique for mass production of nanostructures. Mass production and morphology control of the amorphous helical SiO_2 nanosprings with this technique seem feasible. Further measurements of the mechanical and electrical properties on the nanosprings using nanomanipulation tools with in situ SEM[19] would be highly valuable. Helical nanosprings add a new member to the growing family of one-dimensional nanowires and may find useful applications in nanotechnology.

Acknowledgment. This work was supported by NSF (DMR-0095828) and partly by the laboratory-directed research of Pacific Northwest National Laboratory. The work was performed at the EMSL, a national scientific user facility sponsored by DOE's Office of Biological and Environmental Research and located at Pacific Northwest National Laboratory, operated for DOE by Battelle. Discussions with Drs. Tim Hubler, Scott Lea, and J. S. Young are gratefully acknowledged.

Supporting Information Available: Mean values for the width of the ribbon cross section, the diameter and pitch of the nanosprings as 67, 102, and 85 nm, respectively. This material is available free of charge via the Internet at http://pubs.acs.org.

References

(1) Hu, J.; Odom, T. W.; Lieber, C. M. *Acc. Chem. Res*. **1999**, *32*, 435.
(2) Baughman, R. H.; Zakhidov, A. A.; de Heer, W. A. *Science* **2002**, *297*, 787.
(3) Pan, Z. W.; Dai, Z. R.; Wang, Z. L. *Science* **2001**, *291*, 1947.
(4) Amelinckx, S.; Zhang, X. B.; Bernaerts, D.; Zhang X. F.; Ivanov, V.; Nagy, J. B. *Science* **1994**, *265*, 635.
(5) McIlroy, D. N.; Zhang, D.; Kranov, Y.; Norton, M. G. *Appl. Phys. Lett.* **2001**, *79*, 1540.
(6) Kuzuya, C.; In-Hwang, W.; Hirako, S.; Hishikawa, Y.; Motojima, S. *Chem. Vap. Deposition* **2002**, *8*, 57.
(7) Tang, Y. T.; Zhang, Y. F.; Wang, N.; Lee, C. S.; Han, X. D.; Bello, I.; Lee, S. T. *J. Appl. Phys.* **1999**, *85*, 7981.
(8) Zhang, H. F.; Wang, C. M.; Wang, L. S. *Nano Lett.* **2002**, *2*, 941.
(9) Robbie, K.; Brett, M. J.; Lakhtakia, A. *Nature* **1996**, *384*, 616.
(10) Kennedy, S. R.; Brett, M. J.; Toader, O.; John, S. *Nano Lett*. **2002**, *2*, 59.
(11) Roberts, J. A. *Spring Design and Calculations*; Stechert Hafner Inc.: New York, 1951.
(12) Lacoste, L. *Geophysics* **1983**, *48*, 606.
(13) During the synthesis, the furnace is first raised to 1160 °C under Ar flow while the Si wafer and the sample boats are kept outside. Once the furnace reaches 1160 °C, the Si substrate and the Fe and Si/SiO_2 sample boats are moved to the center of the furnace. At the same time, a CH_4 gas is admitted into the system at a flow rate of 15 mL/min for ~2.0 h. We then turn off the CH_4 flow and the furnace. During the cooling period, the Fe and Si/SiO_2 sample boats are moved away from the center of the furnace. The 2 h reaction time is sufficient to grow a large quantity of nanostructures on the silicon wafer.
(14) Zhang, B.; Wu, Y.; Yang, P.; Liu, J. *Adv. Mater.* **2002**, *14*, 122.
(15) Pan, Z. W.; Dai, Z. R.; Ma, C.; Wang, Z. L. *J. Am. Chem. Soc*. **2002**, *124*, 817.
(16) Yu, D. P.; Hang, Q. L.; Ding, Y.; Zhang, H. Z.; Bai, Z. G.; Wang, J. J.; Zou, Y. H.; Qian, W.; Xiong, G. C.; Feng, S. *Appl. Phys. Lett.* **1998**, *73*, 3076.
(17) Lee, S. T.; Wang, N.; Zhang, Y. F.; Tang, Y. H. *MRS Bull.* **1999**, *24*, 36.
(18) Hu, J. Q.; Jiang, Y.; Meng, X. M.; Lee, C. S.; Lee, S. T. *Chem. Phys. Lett.* **2003**, *367*, 339.
(19) Yu, M. F.; Lourie, O.; Dyer, M. J.; Moloni, K.; Kelly, T. F.; Ruoff, R. S. *Science* **2002**, *287*, 637.

NL0341180